Applied Network Science

CASE STUDY Open Access

Synchronization processes in fNIRS visibility networks

Xhilda Dhamo[1*], Eglantina Kalluçi[1], Eva Noka[1], Gérard Dray[2], Coralie Reveille[2], Stephane Perrey[2], Gregoire Bosselut[2], Darjon Dhamo[3] and Stefan Janaqi[2]

*Correspondence:
Xhilda Dhamo
xhilda.merkaj@fshn.edu.al
[1]Department of Applied Mathematics, Faculty of Natural Sciences, University of Tirana, Tirana, Albania
[2]EuroMov Digital Health in Motion, University of Montpellier, IMT Mines Ales, Montpellier, France
[3]Department of Automation, Faculty of Electrical Engineering, Polytechnic University of Tirana, Tirana, Albania

Abstract

We employ Kuramoto model to assess the presence of synchronization in individuals who fulfill a cooperation task. Our input data is a couple of signals obtained from functional Near-Infrared Spectroscopy Data Acquisition and Pre-processing technology that is used to capture the brain activity of an individual by measuring the oxyhemoglobin (HbO) level. We consider 1 min signal for individuals in three distinct states: (i) rest; (ii) before a disturb happens; (iii) after the disturbance. We estimate global and local order parameters synchronization with the purpose to compare the conditions of reaching a synchronous state in the networks corresponding to different states for distinct individuals and hemispheres of the prefrontal cortices of same individual. Experimental results confirmed once more that coherent state is reached not for same conditions in both individuals and hemispheres of the prefrontal cortices. Furthermore, condition changes even for different events. The computation of the effective frequencies for each degree class indicates clearly the network difference in rest, before and after disturb. Finally, we investigate the dynamic connectivity matrix and consider the similarity between distinct prefrontal cortices over time.

Keywords Visibility graph, Kuramoto model, Complex order parameter, Brain synchronization

Introduction

Collective synchronization phenomena are quite popular in various fields of science and they have been observed in biology, physical, social, technological, neurological sciences for centuries (Pikovsky et al. 2001; Osipov et al. 2007; Arenas et al. 2008; Dörfler and Francesco 2014; Jiruska et al. 2013). It is a complex phenomenon in which large groups of coupled oscillators, with similar natural frequencies, self- synchronize into coherent collective modes of motion and include many variety of biological examples such as congregations of synchronously flashing fireflies, crickets that chirp in unison, an audience clapping at the end of a performance, networks of pacemaker cells in the heart, insulin- secreting cells in the pancreas, as well as neural networks in the brain and spinal cord that control rhythmic behaviors such as breathing, walking and eating (Sherman

and Rinzel 1991; Timme and Wolf 2008; Osipov et al. 2009; Ma and Tang et al. 2015; Ramírez-Ávila et al. 2018). A classical approach to the problem of synchronization consists on modelling each component of the population studied as a phase oscillator. One of the most popular models of coupled phase oscillator is the Kuramoto model (KM), firstly studied in all- to- all coupled oscillators (Acebrón et al. 2005) and years later has been proposed in complex networks (Rodrigues et al. 2016). Researches in this field reflect the importance of KM in describing a wide variety of synchronization processes: phase synchronization (Rosenblum et al. 1996; Arenas et al. 2006a, b; Fell and Axmacher 2011), cluster synchronization (Lu et al. 2010; Pecora et al. 2014; Sorrentino et al. 2016), explosive synchronization (Gómez-Gardeñes et al. 2011; Boccaletti et al. 2016; D'Souza et al. 2019), chimera states (Abram and Strogatz 2004; Wolfrum and Omel'chenko 2011; Schöll 2016) etc. In this paper we are focused on the investigation of the phase synchronization in functional Near-Infrared Spectroscopy Data Acquisition and Pre-processing (fNIRS) visibility networks.

Visibility graphs provide a powerful technique to study time series in the context of complex networks (Lacasa et al. 2008). Through these techniques, time series can be mapped onto complex networks (both directed and undirected; weighted and non-weighted) and their structure and dynamics can be studied by means of the complex networks. Studies on visibility networks have been focused primarily on two distinct directions: (i) canonical dynamics such as stochastic and chaotic processes (Brú et al. 2017; Gonçalves et al. 2016; Lacasa et al. 2009; Luque et al. 2011, 2013); (ii) a feature extraction procedure to make statistical learning (Bhaduri and Ghosh 2016; Hou et al. 2016; Long et al. 2014). In the literature, the reader can find a lot of papers using visibility networks in neuroscience studies: analysis of the electroencephalogram (EEG) data (Mira- Iglesias et al. 2016; Bhaduri and Ghosh 2016); functional magnetic resonance imaging (fMRI) data (Sannino et al. 2017); and fNIRS data (Dhamo et al. 2024).

Inter- brain synchrony in individuals, computed by using the time series of brain signals refers to the dynamical and complex way how two brains communicate and synchronize with each- other during social interaction (Li et al. 2021). Recently, scientists have used fNIRS technology to measure the brain activity of individuals during social interactions and then employing the Wavelet Transform Coherence approach to estimate the synchronization between human brains through the whole time duration of the experiments conducted (Li et al. 2021; Wang et al. 2022). In this paper, we extend our previous study (Dhamo et al. 2024) by modelling the fNIRS data acquisition and pre-processing time series as undirected and unweighted networks employing the visibility criteria and then analyzing the KM in the constructed networks. Here, we are not focused on analyzing the inter- brain synchronization between brains of different individuals, but we consider each individual separately and concentrate in different brain regions of same individual with the purpose to compare the conditions of synchronization in different brain regions. During the time duration of the experiment, the participants passed three different events: (i) rest event, where participants were doing nothing; (ii) before disturbance (five minutes after the beginning of the experiment a disturbance were given to the participants); (iii) after disturbance. The fNIRS technology measured the brain activity (Li et al. 2021) by capturing the oxyhemoglobin (HbO) signals using the optodes positioned in the left and right hemispheres of the prefrontal cortices (PFC) of the participants in the experiment. Our approach consists on three consecutive

moments: (i) firstly, we obtain the brain activity time series from fNIRS technology as described before; (ii) secondly, we model the time series describing the brain activity of one PFC in one specific event as a network by employing the visibility graph technique. This means that each participant will result in two networks for each event (rest, before and after disturbance event); (ii) thirdly, we apply Kuramoto model in all the networks constructed based on the specifications provided in Sect. 3.2 of this study and aim the study at three targets: (i) the computation of the values of the complex order parameter for all networks in each event and compare the values of the coupling strength for which the coherent state between oscillators is reached for different participants and events; (ii) the computation of the effective frequencies within a degree class to describe the evolution of the dynamics for each node in the networks constructed; (iii) the computation of the dynamic connectivity matrix for all networks and evaluating the similarity between connectivity matrices during the simulation time for all combinations of the PFC. To our knowledge, the studies in this field addresses the problem of inter- brain synchronization and does not explore the synchronization phenomena of different brain regions, which is why we have not included a comparative study of our approach to others in this paper.

The Kuramoto model can model the synchronization phenomena in time series, without the need of network representations, however it has its own limitations. Time series analysis focuses on the temporal evolution of individual oscillators, but does not provide insights into how the structure of interactions between these oscillators influences synchronization. Network representations, on the other hand, capture how the arrangements and connections between oscillators affect the synchronization dynamic. Furthermore, when considering large systems of many oscillators, time series may lead to information overloaded, which makes it difficult to capture meaningful patterns, whereas networks can capture this information by using different structural features such as centrality or community structures (Lotfi et al. 2018; Courson et al. 2023). In addition, time series can indicate when and how synchronization happens, but they are less effective at analyzing collective behaviors, like the formation of synchronized clusters or communities of oscillators (Böhm et al. 2010; Favaretto et al. 2017). These are the reasons, why we analyze Kuramoto model on the networks constructed by time series and not directly on time series.

The rest of the paper is organized as follows. In the second section we introduce the visibility graph approach to map time series into networks and its properties and give the mathematics behind the KM in studying synchronization in undirected, unweighted networks. The third section describes the generation of the data used in this study. In addition, we provide the reader with results obtained when studying and analyzing synchronization dynamics using KM in brain activity data. Conclusion summarizes once more all the work conducted and results obtained from our analysis.

Background and methods

Throughout this paper we will refer to a graph (network) as a pair $G = (V, E)$ where V is called the vertex set and E is the edge set. This study is focused only on undirected and unweighted networks with symmetric adjacency matrix A whose entries are $a_{ij} = 1$ if there exists a link between nodes i and j and 0 otherwise (Newman 2018; Estrada and Knight 2015, Barabási and Pósfai 2016; Boccaletti et al. 2006).

We will refer to node degree, the number of edges adjacent to a given node and node degree distribution as the probability distribution of the degrees across all nodes in the network (Newman 2018).

The visibility graph

The construction of the visibility graph is described in detail in (Lacasa et al. 2008, 2009, 2012). Let's consider a time series with N data measured at times $t_i,\ i = 1,\ 2\ ,\ \ldots\ ,\ N$ with values $x_i,\ i = 1,\ 2,\ \ldots\ ,\ N$ and consecutive time points (t_i, x_i), (t_k, x_k) and (t_j, x_j) . Time points (t_i, x_i) and (t_j, x_j) are visible and consequently will become two connected nodes in the visibility graph if for any point (t_k, x_k) between them, they fulfill the following inequation:

$$x_k < x_j + (x_i - x_j)\frac{t_j - t_k}{t_j - t_i} \tag{1}$$

The network, whose nodes fulfill the above condition has four main properties: it is connected, undirected, invariant under affine transformations of the series data and it can be applied to any kind of time series (Lacasa et al. 2008). The construction of visibility graph is illustrated schematically in Fig. 1 given a time series with $N = 20$.

Synchronization dynamic

Synchronization is one of the hottest collective phenomena studied nowadays in complex networks (Boccaletti et al. 2006, 2016). In this study we focus on Kuramoto oscillators where the coupling matrix is a visibility matrix, and provide results referred to phase synchronization in our visibility brain networks.

Initially, we consider an unweighted and undirected network which is composed of N coupled phase-oscillators and the connections among oscillators are described by the adjacency matrix of the network, A which has the value $A_{ij} = 1$ if the oscillators i and j are connected and 0 otherwise. For physicists, the *phase* of a system refers to one of its states. The *phase* is characterized by some physical properties which can be considered as uniform over a macroscopic length scale (Boccaletti et al. 2016). We will denote the *phase* of each oscillator by $\theta_i(t)\ ,\ i = 1,\ 2,\ \ldots\ .,\ N$ and the evolution of each oscillator is described by the Kuramoto model:

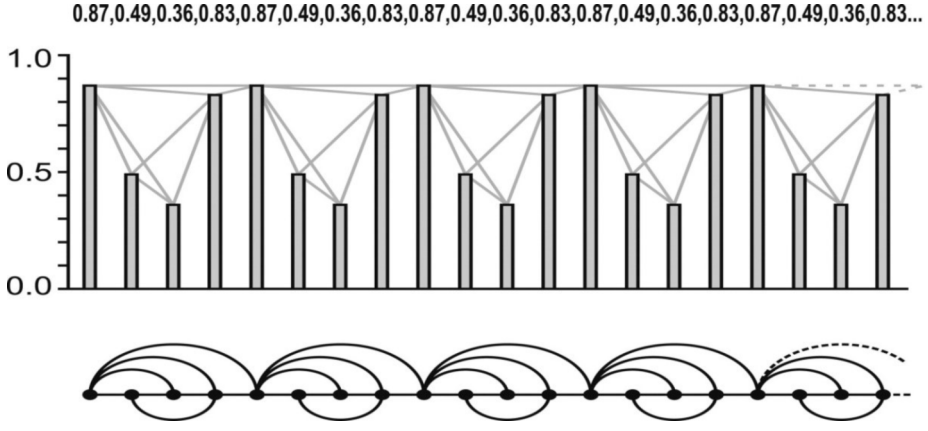

Fig. 1 Construction of visibility graph corresponding to a univariate time series. Adapted from Lacasa et al. (2008)

$$\dot{\theta}_i = \omega_i + \lambda \sum_{j=1}^{N} A_{ij} \sin(\theta_j - \theta_i), \; i = 1, 2, \ldots, N \tag{2}$$

where ω_i represents the natural frequency of the oscillator i and λ refers to the coupling strength of the connections and here it is considered identical for all the connections.

When studying synchronization, we are interested in the transition from the state when the phases of the oscillators are different from each other, thus determining an incoherent state, to the state when all the oscillators have their phases approximately similar and identical (synchronized). This process is referred as *phase transition* and in our problem, it is described by the *complex order parameter* which quantifies the degree of synchronization among N oscillators for increasing values of the coupling strength λ :

$$r(t) e^{i\psi(t)} = \frac{1}{N} \sum_{j=1}^{N} e^{i\theta_j(t)} \tag{3}$$

where $\psi(t)$ stands for the average phase of the collective dynamics of the system and $r(t) \in [0; 1]$ is the degree of synchronization. This is the modulus of the above order parameter, where 0 refers to an incoherent state and 1 refers to a fully synchronized state of the network.

When studying the average value of the order parameter as a function of the coupling strength λ, typically a second-order phase transition occurs, but this depends on the distribution of the natural frequencies. In the next section, we have considered a normal distribution of the natural frequencies with zero mean and unit variance. We will see further that a second-order phase transition is obtained from the incoherent state to the synchronized state.

Although the usage and definition of the complex order parameter is suitable for mean-field models, it does not provide sufficient information about the local dynamic effects. This is the reason that instead of considering a global observable, authors have defined a matrix p of local order parameter which measures the average of the correlation between pairs of oscillators (Arenas et al. 2006a, b):

$$p_{ij} = < \cos(\theta_i(t) - \theta_j(t)) > \tag{4}$$

Where the brackets (< >) stand for the average over initial random phases. Making use of this methodology it is possible to trace the time evolution of pairs of oscillators and to extract information about clusters composed by pairs of oscillators.

After defining the matrix p, a dynamic connectivity matrix is defined as:

$$D_t(T)_{ij} = \begin{cases} 1 & if\ p_{ij} > T \\ 0 & if\ p_{ij} < T \end{cases} \tag{5}$$

Where T is a given threshold, which is used to convert the correlation matrix p to a binary matrix. Different representation of the matrix $D_t(T)$ can be obtained by fixing the time t and moving the value of the threshold T. When increasing the threshold, more disconnected components are created and otherwise, when decreasing the value of the threshold, all the oscillators tend to cluster to the same group. In this study, we fix the value of the threshold T and evolve in time in order to analyze the structure of the dynamic connectivity matrix at various time scales.

In order to analyze in detail the change of the order of the synchronization transition, the effective frequencies are computed which describe the evolution of the dynamics for each node (oscillator) in the network:

$$\omega_i^{eff} = \frac{1}{T}\int_t^{t+T} \dot{\theta}_i(\tau)\, d\tau\,, \quad T \gg 1 \tag{6}$$

Furthermore, one can compute even the evolution of ω_i^{eff} within a degree class k:

$$< \omega >_k = \frac{1}{N_k}\sum_{i:\, k_i=k} \omega_i^{eff} \tag{7}$$

where N_k is the number of nodes with degree k in the network.

Experimental results

Experiment setup

The experiment considered in this study is the same analyzed in our previous paper (Dhamo et al. 2024), but here we consider not only one event, but three events happening during the entire experiment. In summary, there were 18 participants divided into 9 dyads who took part at the cooperative task called "MapTask". The task is described in Fig. 2. Both participants in one dyad had the same icons on their screen, but one of them had a path drawn on its screen, whereas the other one did not have that path. The idea was that the second participants had to draw the same path as the first one, based only on the instruction given by the first participant. From now on, we will refer as the participant *pA* the one who had the path drawn on his screen and *pB* the one who had to draw the same path.

We were interested in the brain activity of the participants during the time- interval of the experiment. The technology used to measure brain activity is fNIRS. Each of the participants had two optodes in their PFC: one positioned in the left hemisphere (hL) and the other in the right hemisphere (hR). These optodes captured the HbO and deoxyhemoglobin (HbR) signals. Considering that the HbO signal is more sensitive to changes in cerebral blood flow than the HbR signal, we focused on the HbO signal (Wang et al. 2022). The dataset used and analyzed in this study is not public, but the reader can assess it by contacting the corresponding author.

Figure 3 illustrates the events of the experiment. The first events was the *Rest* one. No participants did nothing during this event. The time duration of the Rest event slightly

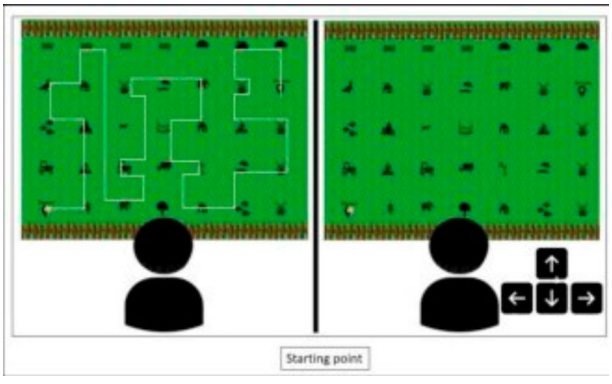

Fig. 2 "MapTask", pA is on the left and pB on the right

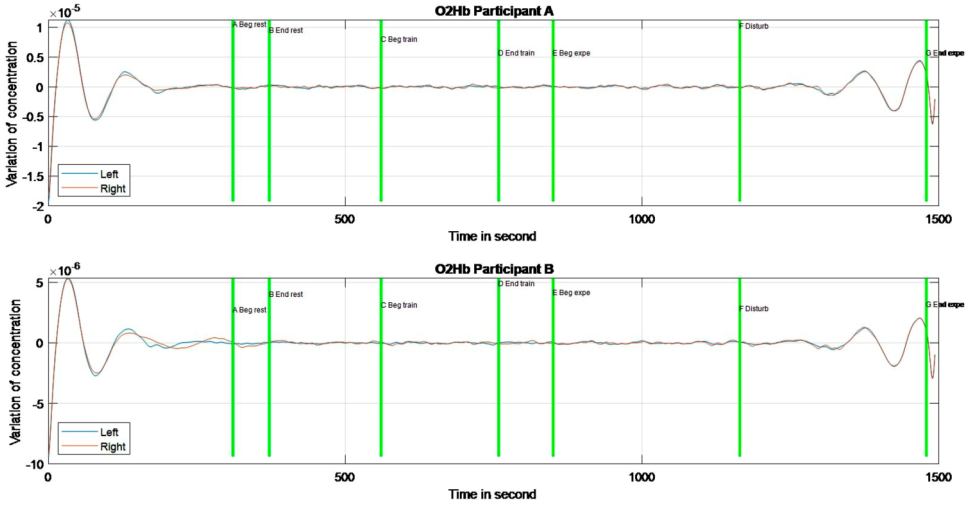

Fig. 3 Rest, train and experiment events for the HbO signals in two participants. Green vertical lines stands for the beginning and ending of each event

differs for different participants, but here we consider the first minute of the event. Furthermore, five minutes after the participants started to give instructions and draw the path, a disturbance was given to them. Their screen disappeared immediately for a short time and then appeared again. In our previous study (Dhamo et al. 2024) we consider only the five minutes before the disturbance happened, but here we extend our study and consider the HbO signals in the time intervals one minute from the beginning of the rest event, one minute before disturb and one minute after disturb. Our intention is to analyze the phase synchronization and conditions for which an explosive synchronization is present in different participants, in different events and in different PFCs of the same participants.

Kuramoto model in fNIRS networks

The HbO signals measured at different events (described in Sect. 3.1) were mapped into visibility networks following Lacasa et al. (2008). Since, the time duration is one minute in each of the events considered; all the visibility networks have the same number of nodes (613 nodes). From now on, we will refer as lPFC (rPFC) to signals measured in the left (right) prefrontal cortex hemispheres; pAhL (pAhR) the signals measured at the left (right) prefrontal cortex hemisphere of the participant pA; pBhL (pBhR) the signals measured at the left (right) cortex hemisphere of the participant pB.

In this section we consider natural frequencies from normal distribution with zero mean and unit variance. The Kuramoto model is executed for all the networks constructed and obtained the evolution of the phases $\theta_i,\ i = 1,\ 2,\ \ldots .,\ 613$ for all the networks for different values of the coupling strengths. The value of the coupling strength needed to obtain the stationary state depend on different networks. In Rest networks, the values of the coupling strength are taken from interval $[0; 1]$ with step of 0.01. The complex order parameter is computed using Eq. (2) within the stationary state. Since the natural frequencies are taken randomly, we repeat the execution of the Kuramoto model 20 times for each network and then computed the final complex order parameter as the average of the order parameters obtained in each execution. The model is programmed

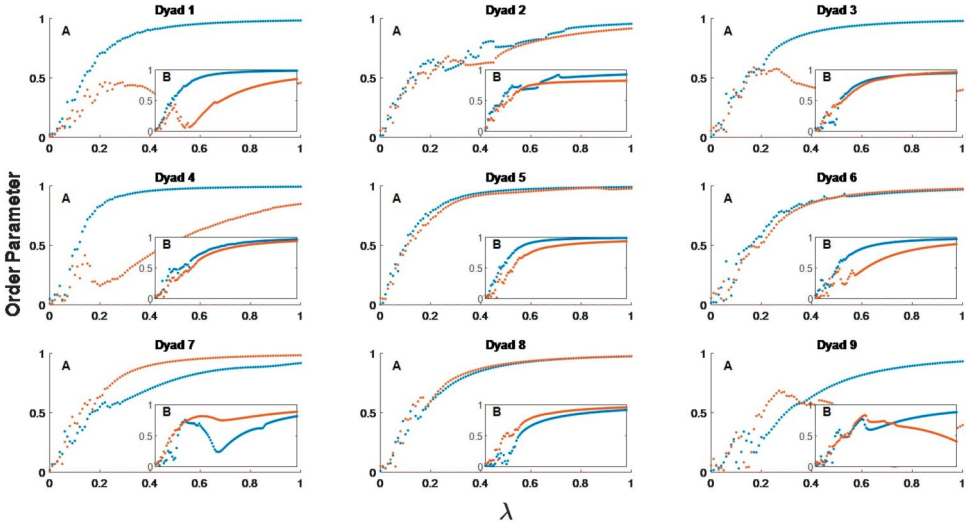

Fig. 4 Complex order parameter in *Rest* networks. **A** refers to pA and **B** pB. The main plot illustrates the order parameter for pA and inset for pB. Blue color stands for hL and red color for hR

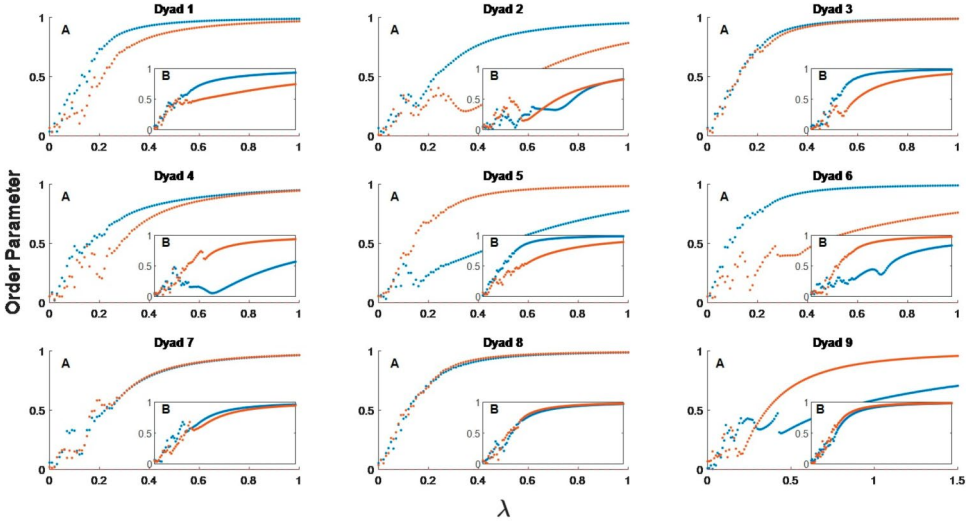

Fig. 5 Complex order parameter in *Before Disturb* networks. **A** refers to pA and **B** pB. The main plot illustrates the order parameter for pA and inset for pB. Blue color stands for hL and red color for hR

in Matlab and we use Runge-Kuta 4-th order to solve numerically systems of differential equations.

The results of the complex order parameter computed for networks in the (i) rest; (ii) before disturb; and (iii) after disturb events are illustrated in Figs. 4, 5 and 6 respectively. It is observed that in the 78% of the *After Disturb* networks, it is needed a bigger value of the coupling strength to obtain the coherent state between oscillators compared to the *Rest* and *Before Disturb* networks. The *Rest* networks corresponding to the hL (Dyad 1, 2, 3, 4, 5, 6, 9) achieve the coherent state for smaller values of the coupling strength then the *Rest* networks corresponding to hR in both pA and pB. There is a big change between the phase- transition of the hL and hR for pA in Dyad 1, 3, 4, and 9 from the incoherent state up to the stationary state. In Dyad 9 both lines in pA and pB intersect each other: for small values of the coupling strength the hR provide a higher value of

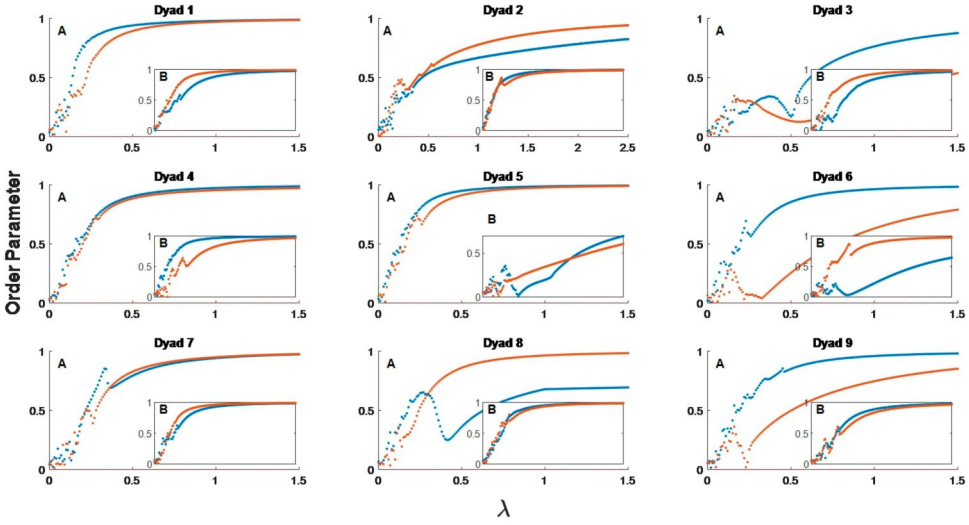

Fig. 6 Complex order parameter in *After Disturb* networks. **A** refers to pA and **B** pB. The main plot illustrates the order parameter for pA and inset for pB. Blue color stands for hL and red color for hR

the order parameter then the hL, but when increasing the coupling strength only the hL reaches the stationary state. So, the hR in Dyad 9, Dyad 3 pA and Dyad 1 pA does not reach the stationary state for value of the coupling strength up to the value 1.5.[1]

Comparing the phase transitions between rest and before disturb networks, it is evident that they do not follow the same evolution. In Dyads 2, 5 and 6 there is a significant change between the values of coupling strength for which synchronization is achieved in rest and before disturb networks. On the other hand, Dyad 8 present approximately the same transition to the stationary state in both states, whereas for the other dyads the change between the coupling strength of different hemispheres becomes smaller.

Considering the networks after disturbance, the results show that in Dyad 3 for both pAhL and pAhR and pAhL in Dyad 8, the phase transition curve does not exhibit a monotonic increasing evolution toward the stationary state at low values of the coupling strength.

Furthermore, we have computed the effective frequencies based on Eq. (7) within a degree class, which describe the evolution of the dynamics for each node in the network. Figure 7 illustrates the effective frequencies for all pAhL Rest networks, whereas for the other networks the graphical results are provided in the ***supplementary material 1.***

The effective frequencies related to networks corresponding to signals in Rest event tend to reach the coherent state faster than the networks corresponding to before and after disturb. In the Rest network the coherent state is achieved approximately at the same small values of λ . The nodes in the network with higher degree tend to reach faster the stationary state. Whereas in Before disturb network (see supplementary material 1) the graphical representations of the effective frequency have a different look. This nodes with high and low degree become coherent for small values of the coupling strength, but it requires increasing the coupling strength to reach the stationary state. This is in contrast with Rest networks where the stationary state is reached without as much oscillations as in Before disturb networks. On the other hand, in the After disturb networks

[1] We have visualized the phase transitions lines for values of the coupling strength from 0 to 1 with step 0.01, but for the other analyzes we have increased the value of the coupling strength until the stationary state is reached for all networks and then computing the effective frequencies and similarities.

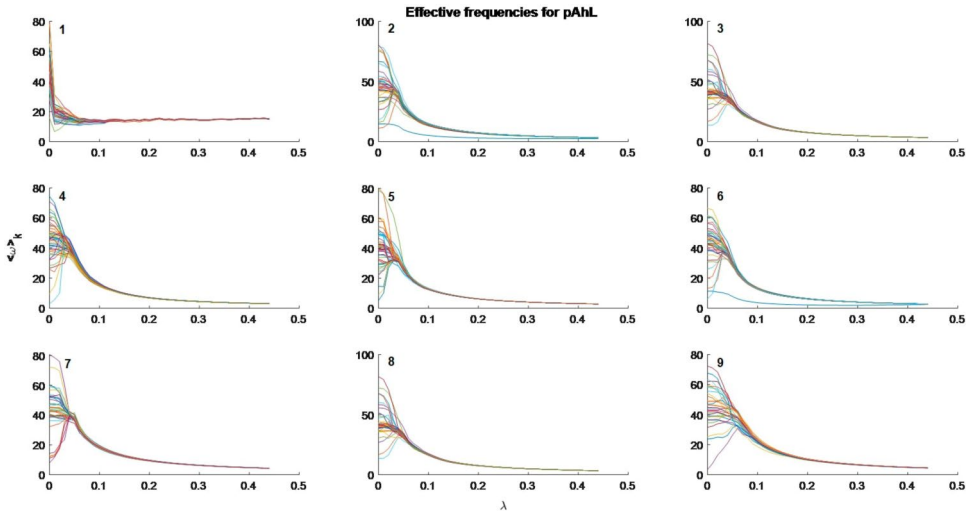

Fig. 7 Effective frequencies related to the pAhL networks considering all dyads. Numbers positioned in upper left of each figure correspond to the number of a dyad

some dyads reveal the same properties as in the Rest networks and some other as in the Before disturb networks. We relate these effects with the fact that in Before disturb event the human brain is performing a cognitive task and has an activity to deal with, whereas in the rest event, the human brain is just resting. Considering the after disturb results, there are some dyads which were affected more and some other less from the disturbance given in the experiment. The effective frequencies corresponding to After disturb events for dyads 3, 4, 5, and 8 display the same evolution as for rest event. These dyads did not have a strong impact from the disturbance in contrast from dyads 1, 2, 6, and 7 which display a similar evolution as in before disturb event.

Based on Eqs. (4) and (5) we computed the dynamic connectivity matrix for all networks. Our interest is to study the similarity between connectivity matrix during the simulation time for combinations:

1. pAhL-pAhR.
2. pBhL-pBhR.
3. pAhL-pBhL.
4. pAhL-pBhR.
5. pAhR-pBhL.
6. pAhR-pBhR.

We employ the mean-square error (MSE) measure to evaluate the similarity between two adjacency matrices corresponding to two distinct network. A lower MSE value indicates greater similarity between two adjacency matrices. Taking into account all the combinations presented in Figs. 8 and 9, and 10, it is clear that the dynamic connectivity matrices initially exhibit dissimilarity, followed by a decrease in the MSE coefficient. However, as the simulation time progresses, the MSE coefficient begins to rise.

Conclusions

In this paper we studied the brain synchronization problem employing the Kuramoto model in complex networks. The fNIRS technology was used to measure the brain activity during cognitive task for 9 dyads in three distinct states. We considered in total 36

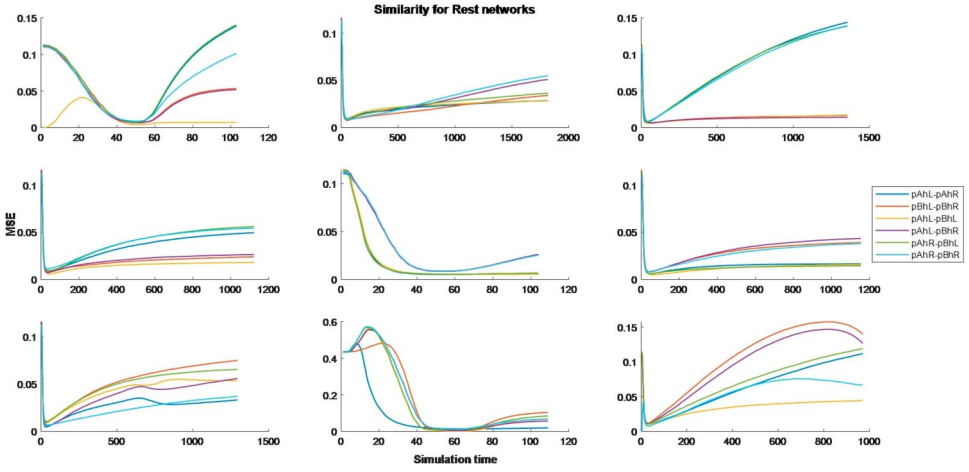

Fig. 8 Similarity in the Rest dynamic connectivity matrices

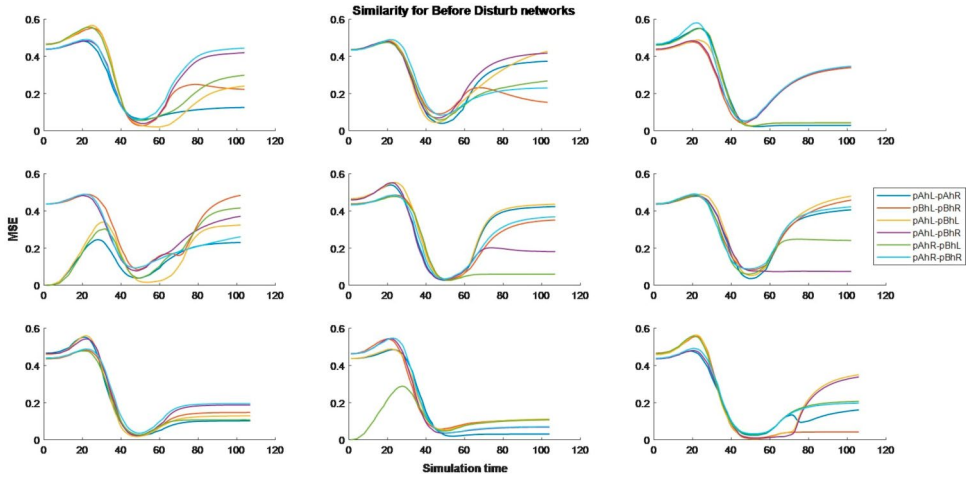

Fig. 9 Similarity in the Before Disturb dynamic connectivity matrices

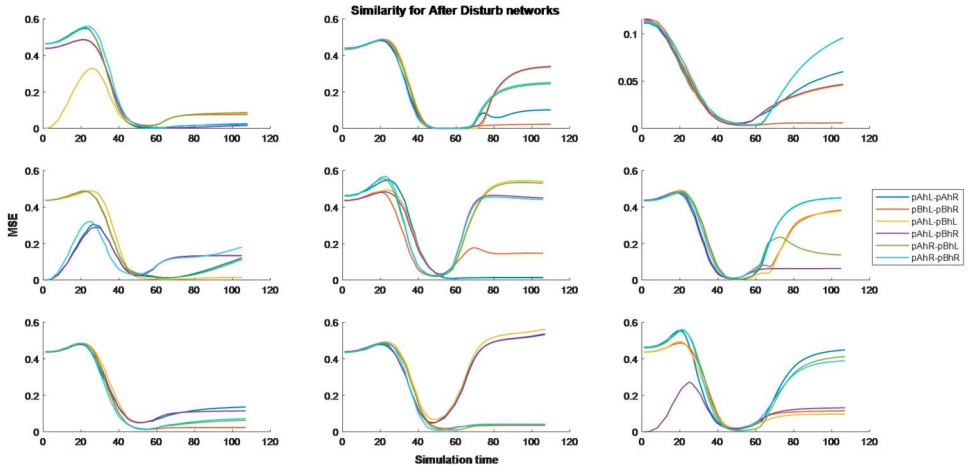

Fig. 10 Similarity in the After Disturb dynamic connectivity matrices

fNIRS signals. In addition, the visibility graph approach is used to convert signals onto networks. Furthermore, we analyse the conditions for which a coherent state is reached based on global order parameters (complex order parameters) and on local order parameters (dynamics connectivity matrix). Analysing the values of the complex order parameters versus the values of coupling strength, we confirmed our previous paper results (Dhamo et al. 2024) that the synchronization state is not reached for the same conditions, not only for different individuals, but also for different prefrontal cortices of the same individual. Furthermore, the conditions change even in different states of the experiment. The computation of the effective frequencies clearly shows the difference between different events. In this paper, we do not study the effects of structural components of the networks in the occurrence of the synchronization phenomena both theoretical and experimental, but this is our goal for future work. However, we have presented the results related to structural aspects of fNIRS visibility networks in the 'before disturb' event at the final Conference of the COST Action "Mathematical models for interacting dynamics on networks". As far as we know, there does not exists any paper till now which describes in details the fNIRS visibility networks topology and provide insights on the impacts of structural components of these kind of networks in dynamic processes.

Supplementary Information

The online version contains supplementary material available at https://doi.org/10.1007/s41109-024-00663-x.

Supplementary Material 1

Acknowledgements
We would like to thank Profesor Sergio Gomez from University Rovira I Virgili, Tarragona, Spain for his valuable help and information shared with us and Guilhem Belda, President of the Semaxone company (Rochefort-du-Gard, France), for his help in developing the application and providing the audio equipment.

Author contributions
All the authors contributed equally to this work.

Funding
This study is supported by Research Expertise from the Academic Diaspora (READ) project titled "Optimization and Operational Research in Data Science" from Albanian-American Development Foundation (AADF).

Data availability
The datasets used and/or analysed during the current study are available from the corresponding author on reasonable request.

Declarations

Ethics approval and consent to participate
Not applicable.

Consent for publication
Not applicable.

Competing interests
The authors declare no competing interests.

Received: 29 April 2024 / Accepted: 18 August 2024
Published online: 02 September 2024

References

Abrams DM, Strogatz SH (2004) Chimera States for coupled oscillators. Phys Rev Lett 93. https://doi.org/10.1103/PhysRevLett.93.174102
Acebrón JA, Bonilla LL, Vicente CJP et al (2005) The Kuramoto model: a simple paradigm for synchronization phenomena. Rev Mod Phys. https://doi.org/10.1103/RevModPhys.77.137. 77:

Arenas A, Díaz-Guilera A, Pérez-Vicente CJ (2006a) Synchronization processes in complex networks. Physica D 224:27–34. https://doi.org/10.1016/j.physd.2006.09.029
Arenas A, Díaz-Guilera A, Pérez-Vicente CJ (2006b) Synchronization reveals topological scales in Complex Networks. Phys Rev Lett. https://doi.org/10.1103/PhysRevLett.96.114102. 96:
Arenas A, Díaz-Guilera A, Kurths J et al (2008) Synchronization in complex networks. Phys Rep 469:93–153. https://doi.org/10.1016/j.physrep.2008.09.002
Barabási A-L, Pósfai M (2016) Network Science, 1st edn. Cambridge University Press
Bhaduri A, Ghosh D (2016) Quantitative Assessment of Heart Rate Dynamics during Meditation: an ECG based study with multifractality and visibility graph. Front Physiol. https://doi.org/10.3389/fphys.2016.00044. 7:
Boccaletti S, Latora V, Moreno Y et al (2006) Complex networks: structure and dynamics. Phys Rep 424:175–308. https://doi.org/10.1016/j.physrep.2005.10.009
Boccaletti S, Almendral JA, Guan S et al (2016) Explosive transitions in complex networks' structure and dynamics: Percolation and synchronization. Phys Rep 660:1–94. https://doi.org/10.1016/j.physrep.2016.10.004
Böhm C, Plant C, Shao J, Yang Q (2010) Clustering by synchronization. pp 583–592
Brú A, Gómez-Castro D, Nuño JC (2017) Visibility to discern local from nonlocal dynamic processes. Physica A 471:718–723. https://doi.org/10.1016/j.physa.2016.12.078
Courson J, Manos T, Quoy M (2023) Networks' Modulation: How Different Structural Network Properties Affect the Global Synchronization of Coupled Kuramoto Oscillators. In: Springer Proceedings in Complexity. Springer
D'Souza RM, Gómez-Gardeñes J, Nagler J, Arenas A (2019) Explosive phenomena in complex networks. Adv Phys 68:122–223. https://doi.org/10.1080/00018732.2019.1650450
Dhamo X, Kalluçi E, Dray G et al (2024) Global synchronization measure Applied to brain signals data. In: studies in Computational Intelligence. Springer, France
Ding D, Tang Z, Wang Y, Ji Z (2020) Synchronization of nonlinearly coupled complex networks: distributed impulsive method. Chaos Solitons Fractals. https://doi.org/10.1016/j.chaos.2020.109620. 133:
Dörfler F, Francesco B (2014) Synchronization in complex networks of phase oscillators: a survey. Automatica 50:1539–1564. https://doi.org/10.1016/j.automatica.2014.04.012
Estrada E, Knight PA (2015) A first course in Network Theory. Oxford University Press
Favaretto C, Cenedese A, Pasqualetti F (2017) Cluster synchronization in networks of Kuramoto Oscillators. IFAC-PapersOnLine 50:2433–2438. https://doi.org/10.1016/j.ifacol.2017.08.405
Fell J, Axmacher N (2011) The role of phase synchronization in memory processes. Nat Rev Neurosci 12. https://doi.org/10.1038/nrn2979
Gómez-Gardeñes J, Gómez S, Arenas A, Moreno Y (2011) Explosive synchronization transitions in scale-free networks. Phys Rev Lett 106. https://doi.org/10.1103/PhysRevLett.106.128701
Gonçalves BA, Carpi L, Rosso OA, Ravetti MG (2016) Time series characterization via horizontal visibility graph and information theory. Physica A 464:93–102. https://doi.org/10.1016/j.physa.2016.07.063
Hou FZ, Li FW, Wang J, Yan FR (2016) Visibility graph analysis of very short-term heart rate variability during sleep. Physica A 458:140–145. https://doi.org/10.1016/j.physa.2016.03.086
Jiruska P, de Curtis M, Jefferys JGR et al (2013) Synchronization and desynchronization in epilepsy: controversies and hypotheses. J Physiol 591:787–797. https://doi.org/10.1113/jphysiol.2012.239590
Lacasa L, Luque B, Ballesteros F et al (2008) From time series to complex networks: the visibility graph. Appl Math 105:4972–4975. https://doi.org/10.1073/pnas.0709247105
Lacasa L, Luque B, Luque J, Nuño JC (2009) The visibility graph: a new method for estimating the Hurst exponent of fractional brownian motion. Europhys Lett 86. https://doi.org/10.1209/0295-5075/86/30001
Lacasa L, Nuñez A, Roldán É et al (2012) Time series irreversibility: a visibility graph approach. Eur Phys J B 85
Lacasa L, Nicosia V, Latora V (2015) Network structure of multivariate time series. Sci Rep 5:. https://doi.org/https://doi.org/10.1038/srep15508
Li R, Mayseless N, Balters S, Reiss AL (2021) Dynamic inter-brain synchrony in real-life inter-personal cooperation: a functional near-infrared spectroscopy hyperscanning study. NeuroImage 238
Liu H, Li J, Li Z et al (2022) Intralayer Synchronization of Multiplex Dynamical
Long X, Fonseca P, Aarts RM et al (2014) Modeling cardiorespiratory interaction during human sleep with complex networks. Appl Phys Lett 105. https://doi.org/10.1063/1.4902026
Lotfi N, Rodrigues FA, Darooneh AH (2018) The role of community structure on the nature of explosive synchronization. https://doi.org/10.1063/1.5005616. Chaos 28:
Lu W, Liu B, Chen T (2010) Cluster synchronization in networks of coupled nonidentical dynamical systems. https://doi.org/10.1063/1.3329367. Chaos 20:
Luque B, Lacasa L, Ballesteros F, Robledo A (2011) Feigenbaum Graphs: a Complex Network Perspective of Chaos. PLoS ONE 6:1–8
Luque B, Ballesteros F, Núñez AM, Robledo A (2013) Quasiperiodic graphs: Structural Design, Scaling and Entropic properties. J Nonlinear Sci 23:335–342. https://doi.org/10.1007/s00332-012-9153-2
Ma J, Tang J (2015) A review for dynamics of collective behaviors of network of neurons. Sci China Technological Sci 58:2038–2045. https://doi.org/10.1007/s11431-015-5961-6
Mira- Iglesias A, Conejero JA, Navarro-Pardo E (2016) Natural visibility graphs for diagnosing attention deficit hyperactivity disorder (ADHD). Electron Notes Discrete Math 54:337–342
Networks via Pinning Impulsive Control IEEE Trans Cybernetics 52:2110–2122. https://doi.org/10.1109/TCYB.2020.3006032
Newman M (2018) Networks, Second Edition. Oxford University Press
Osipov GV, Kurths J, Zhou C (2007) Synchronization in Oscillatory Networks
Osipov GH, Kanakov OI, Chan C-K et al (2009) Synchronization phenomena in networks of Oscillatory and Excitable Luo-Rudy cells. Complex Dynamics in physiological systems: from heart to Brain. Understanding Complex systems. Springer, Dordrecht
Pecora LM, Sorrentino F, Hagerstrom AM et al (2014) Cluster synchronization and isolated desynchronization in complex networks with symmetries. Nat Commun. https://doi.org/10.1038/ncomms5079. 5:
Pikovsky A, Rosenblum M, Kurths J (2001) Synchronization. Cambridge University Press

Ramírez-Ávila GM, Kurths J, Depickère S, Deneubourg J-L (2018) Modeling Fireflies Synchronization. A Mathematical Modeling Approach from Nonlinear Dynamics to Complex Systems Nonlinear Systems and Complexity 22:. https://doi.org/10.1007/978-3-319-78512-7_8
Rodrigues FA, Peron TKDM, Ji P, Kurths JG (2016) The Kuramoto model in complex networks. Phys Rep 610:1–98
Rosenblum MG, Pikovsky AS, Kurths J (1996) Phase synchronization of chaotic oscillators. Phys Rev Lett 76
Sannino S, Stramaglia S, Lacasa L, Marinazzo D (2017) Visibility graphs for fMRI data: Multiplex temporal graphs and their modulations across resting-state networks. Netw Neurosci 1:208–221
Schöll E (2016) Synchronization patterns and chimera states in complex networks: interplay of topology and dynamics. Eur Phys J Special Top 225:891–919. https://doi.org/10.1140/epjst/e2016-02646-3
Sherman A, Rinzel J (1991) Model for synchronization of pancreatic beta-cells by gap junction coupling. Biophys J. https://doi.org/10.1016/S0006-3495(91)82271-8. 59:
Sorrentino F, Pecora LM, Hagerstrom AM et al (2016) Complete characterization of the stability of cluster synchronization in complex dynamical networks. Sci Adv. https://doi.org/10.1126/sciadv.1501737. 2:
Supriya S, Siuly S, Wang H et al (2016) Weighted visibility graph with Complex Network Features in the detection of Epilepsy. IEEE Access 6554–6566. https://doi.org/10.1109/ACCESS.2016.2612242
Tang Y, Qian F, Gao H, Kurths J (2014) Synchronization in complex networks and its application – a survey of recent advances and challenges. Annu Rev Control 38:184–198. https://doi.org/10.1016/j.arcontrol.2014.09.003
Timme M, Wolf F (2008) The simplest problem in the collective dynamics of neural networks: is synchrony stable? https://doi.org/10.1088/0951-7715/21/7/011. Nonlinearity 21:
Wang X, Zhang Y, He Y et al (2022) Dynamic Inter-brain Networks Correspond with Specific Communication behaviors: using Functional Near-Infrared Spectroscopy Hyperscanning during Creative and non-creative communication. Front Hum Neurosci 16. https://doi.org/10.3389/fnhum.2022.907332
Wolfrum M, Omel'chenko OE (2011) Chimera states are chaotic transients. Phys Rev E. https://doi.org/10.1103/PhysRevE.84.015201. 84:
Zhang J, Small M (2006) Complex Network from Pseudoperiodic Time Series: Topology versus Dynamics. Phys Rev Lett 96. https://doi.org/10.1103/PhysRevLett.96.238701
Zhang X, Boccaletti S, Guan S, Liu Z (2015) Explosive synchronization in adaptive and multilayer networks. Phys Rev Lett 114
Zheng M, Domanskyi S, Piermarocchi C, Mias GI (2021) Visibility graph based temporal community detection with applications in biological time series. https://doi.org/10.1038/s41598-021-84838-x. Scientific Reports 11:

Publisher's note